

Assessing the Strategic Preparation of CPPs: A Computational Analysis of the Impact of Different Catechol-Based Ligands [†]

Matías Capurso, Gabriel Radivoy, Fabiana Nador and Viviana Dorn *

Instituto de Química del Sur (INQUISUR-CONICET), Departamento de Química, Universidad Nacional del Sur, Av. Alem 1253, Bahía Blanca B8000CPB, Argentina; matias.capurso@uns.edu.ar (M.C.); email1@email.com (G.R.); email1@email.com (F.N.)

* Correspondence: vdorn@uns.edu.ar

[†] Presented at the 27th International Electronic Conference on Synthetic Organic Chemistry (ECSOC-27), 15–30 November 2023; Available online: <https://ecsoc-27.sciforum.net/>.

Abstract: DFT calculations were applied to an iron/catechol derivatives system to investigate the effect on the structure of CPPs as a function of (a) metal valence, Fe⁺² and Fe⁺³ in high and low spin states; (b) type of chelating groups in the catechol derivatives and their geometries; and (c) the aliphatic chain length between two chelating groups in a model polydentate ligand. The results indicate that catechol-pyridine and bis-catechol ligands, with Fe⁺³ salts, are the promising combinations to synthesize CPPs. In addition, the inclusion of an aliphatic chain with 4 carbons between the chelating groups could enhance polymerization versus monomer formation.

Keywords: CPPs; catechol; DFT

1. Introduction

Catechol derivatives are promising for functional materials [1] due to their metal-chelating ability [2], making them excellent ligands for generating Coordination Polymer Particles (CPPs). They self-assemble into CPPs from metal ions and polydentate organic ligands (Figure 1) [3]. Up till now polymeric structure characterization remains challenging, and, on the other hand, being able to predict the CPPs properties such as morphology, size and stability in diverse environments is essential for their applications.

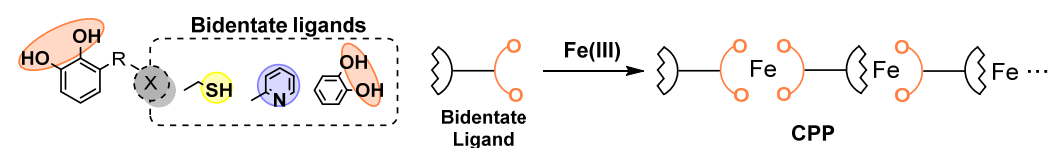


Figure 1. Formation of CPPs.

In this study, we present the findings from conducting DFT calculations on iron/catechol-derivative systems with the primary functional groups being considered for use in CPPs synthesis (Figure 1). We then conducted an analysis of the results to better understand their impact on the CPPs synthesis process.

2. Methods

All computations in this work were carried out with the ORCA 5.0 program package [4]. Geometry optimizations of the high spin and low spin states for each complex were performed with the BP86 density functional [5] with D3BJ dispersion correction [6], being a methodology widely used for this type of complexes [7]. Single point energy calculations were carried out with wb97X [8] with D3BJ dispersion correction. The def2 TZVPP

Citation: Capurso, M.; Radivoy, G.; Nador, F.; Dorn, V. Assessing the Strategic Preparation of CPPs: A Computational Analysis of the Impact of Different Catechol-Based Ligands. *Chem. Proc.* **2023**, *14*, x. <https://doi.org/10.3390/xxxxx>

Academic Editor(s): Name

Published: 15 November 2023



Copyright: © 2023 by the authors. Submitted for possible open access publication under the terms and conditions of the Creative Commons Attribution (CC BY) license (<https://creativecommons.org/licenses/by/4.0/>).

(Fe), TZVP (O, N, S) and SVP (other) basis sets [9] were applied in the geometry optimizations and single point calculations.

3. Results and Discussion

The synthesis and properties of CPPs are highly dependent on the type of metal ion used, the chelating groups present in the ligands and their structure. In this context, by employing DFT calculations on an iron/catechol derivative system, we pretend to investigate the effect on the structure of CPPs based on:

- The use of Fe^{+3} and Fe^{+2} in high and low spin states;
- The type of chelating groups in catechol derivatives as well as their geometries;
- The aliphatic chain length between the two chelating groups in a model polydentate ligand.

3.1. Analysis of Metallic Species and Organic Chelating Groups

As previously mentioned, the formation of iron complexes with simplified representative structures of the ligands (see the structures in Table 2) and the Fe^{+2} and Fe^{+3} species in high and low spin states were considered. It is known that other Fe^{+3} complexes with catechol derivatives are known to exhibit high-spin ferric species [10], and we found the same trend, all the high-spin Fe^{+3} complexes were approximate 20 kcal/mol energetically more stable than that their low-spin counterparts (Table 1). A comparable trend was observed for those Fe^{+2} complexes.

Table 1. High-Low Spin energy differences (kcal/mol) for the iron complexes.

Complex	Fe+3	Fe+2
<i>trans</i> -Fe(cat) ₂ (pyr) ₂	-12	-21
<i>cis</i> -Fe(cat) ₂ (pyr) ₂	-22	-18
Fe(cat) ₂	-21	-25
Fe(cat) ₃	-28	-45
<i>trans</i> -Fe(cat) ₂ (thiol) ₂	-21	-34
<i>cis</i> -Fe(cat) ₂ (thiol) ₂	-24	-57

In a subsequent step, the binding energies for the high-spin iron complexes were evaluated and the results are compared in Table 2. According to the results, Fe^{+3} complexes were more stable than Fe^{+2} complexes, with binding energies approximately twice as high. As can be seen from Table 2, for the *trans*-Fe[(cat)₂(pyr)₂] complexes, the Fe^{+3} complex, has a binding energy of 1609 kcal/mol, whereas the Fe^{+2} analog has a binding energy of 848 kcal/mol.

Table 2. Binding energy of high-spin iron complexes (kcal/mol).

Metallic ion	[Fe(cat) ₂ (pyr) ₂]		[Fe(cat) ₂]		[Fe(cat) ₃]	[Fe(cat) ₂ (thiol) ₂]	
	<i>trans</i>	<i>cis</i>	<i>tetrahedral</i>	<i>planar</i>		<i>trans</i>	<i>cis</i>
Fe^{+3}	-1609	-1602	-1582	-1569	-1558	-1455	-1460
Fe^{+2}	-848	-838	-832	-831	-648	-546	-570

Considering the binding energy of high-spin Fe^{+3} complexes, it was observed that those with catechol-pyridine as ligands were more stable, favoring the *trans* geometry

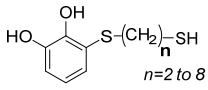
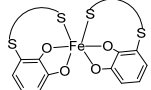
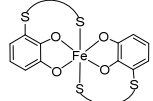
(1609 kcal/mol) over the *cis* (1602 kcal/mol) by 7 kcal/mol. Fe(cat)₂ and Fe(cat)₃ complexes followed them in stability, whereas catechol-thiol complexes proved to be the least stable, as can be seen in Table 2. The same trend was observed for Fe⁺² complexes.

Based on these results, we could assume that the use of Fe(III) salts in combination with catechol-pyridine or bis-catechol ligands, appears to be the most appropriate combination for the synthesis of CPPs.

3.2. Effect of the Methylene Spacers between the Chelating Groups

On the other hand, to examine the influence of the aliphatic chain length between the two chelating groups, a ligand model 3-((5-mercaptoalkyl)thio)benzene-1,2-diol was used, with the alkyl chain ranging from 2 to 8 methylene groups (Table 3). The length and conformation of this alkylic chain could significantly affect the formation of the CPPs, as it may precipitate as stable monomer, thereby inhibiting polymer growth.

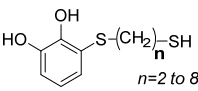
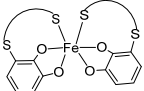
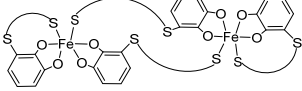
Table 3. Structure of the model ligand and relative binding energies of the *cis* and *trans* monomers.

 model ligand n=	 <i>cis</i>-monomer (kcal/mol)	 <i>trans</i>-monomer (kcal/mol)	ΔE=E_{cis}-E_{trans} (kcal/mol)
2	no formation	no formation	-
3	0	5	-5
4	16	21	-5
6	29	34	-6
8	46	50	-4

We calculated the formation of the possible *cis* and *trans* isomers of the monomers between high-spin Fe⁺³ and the model ligand. As can be observed from Table 3, to obtain both, *cis*- and *trans*-monomers, were necessary at least three methylene groups as alkyl spacer in the alkyl chain. Additionally, the *cis* complexes were approximately 5 kcal/mol more stable than the *trans* complexes. It is also observed that as the methylene spacer decreases in length, the monomers increase their stability. For the *cis* isomer, Table 3 shows an energy stabilisation of 46 kcal/mol when methylene groups reducing from 8 to 3, and 50 kcal/mol for the *trans* isomer.

The same analysis was carried out to examine the dimers formation, and their relative energy values are presented in Table 4. It was found that dimer formation was more favorable for 4 methylene groups in the alkyl chain. On the other hand, isolated monomers showed to be more energetically stable compared to the respectively dimers; however, as the length alkylic chain increases, the formation of the dimers becomes progressively more favorable.

Table 4. Structure of the Model ligand and relative binding energies of cis monomer and dimer.

 model ligand n=	 cis-monomer (kcal/mol)	 dimer (kcal/mol)	$\Delta E = E_{\text{dim}} - E_{\text{mon}}$ (kcal/mol)
3	0	11	11
4	16	0	-16
6	29	20	-8
8	46	39	-6

According to the obtained results, we could assume that the incorporation of an alkyl spacer of at least 4 methylene groups between the chelating groups could advantage the polymer formation over the monomers formation, thus favoring the synthesis of the CPPs.

The structures are currently being recalculated by incorporating solvent and other metal ions, both of which are factors that can affect the energy and/or structure of the CPPs.

4. Conclusion

DFT calculations are a powerful tool for investigating the structure and properties of CPPs. Base on the findings, catechol-pyridine and bis-catechol ligands, with Fe³⁺ as metallic ion, would form structures potentially suitable for synthesizing CPPs.

The analysis on the effect of the methylene spacers between the chelating groups could indicates that a shorter spacer, of at least three methylenes, promotes the monomer formation, while increasing the spacer to four or more methylenes, improves the possibility of polymerization.

Future research are focus on the impact of additional factors on the structure of CPPs, such as the presence of solvent molecules and other metallic ions.

Author Contributions: V.D. carried out the conceptualization, investigation, methodology and writing; F.N. participated in the investigation, methodology and writing; M.C. participated in the methodology; G.R. carried out the funding acquisition, the project administration, investigation and writing. All authors have read and agreed to the published version of the manuscript.

Funding: This work was generously supported by the Consejo Nacional de Investigaciones Científicas y Técnicas (CONICET, PIP N° 11220200101665CO), Agencia Nacional de Promoción Científica y Tecnológica (ANPCyT, PICT 2018-2471) and Universidad Nacional del Sur (UNS, PGI 24/Q106) from Argentina.

Data Availability Statement: Data available upon request.

Acknowledgments: M.C. thanks the ANPCyT for a doctoral fellowship.

Conflicts of Interest: The authors declare no conflict of interest.

References

- Zhang, W.; Wang, R.; Sun, Z.; Zhu, X.; Zhao, Q.; Zhang, T.; Cholewinski, A.; Yang, F.; Zhao, B.; Pinnaratip, R.; et al. Catechol-Functionalized Hydrogels: Biomimetic Design, Adhesion Mechanism, and Biomedical Applications. *Chem. Soc. Rev.* **2020**, *49*, 433–464. <https://doi.org/10.1039/C9CS00285E>.
- Saiz-Poseu, J.; Mancebo-Aracil, J.; Nador, F.; Busqué, F.; Ruiz-Molina, D. The Chemistry behind Catechol-Based Adhesion. *Angew. Chem. Int. Ed.* **2019**, *58*, 696–714. <https://doi.org/10.1002/anie.201801063>.
- Suárez-García, S.; Solórzano, R.; Novio, F.; Alibés, R.; Busqué, F.; Ruiz-Molina, D. Coordination Polymers Nanoparticles for Bioimaging. *Coord. Chem. Rev.* **2021**, *432*, 213716. <https://doi.org/10.1016/j.ccr.2020.213716>.
- (a) Neese, F. The ORCA Program System. *WIREs Comput. Mol. Sci.* **2012**, *2*, 73–78. <https://doi.org/10.1002/wcms.81>. (b) Neese, F. Software Update: The ORCA Program System—Version 5.0. *WIREs Comput. Mol. Sci.* **2022**, *12*, e1606. <https://doi.org/10.1002/wcms.1606>.

5. Perdew, J.P. Density-Functional Approximation for the Correlation Energy of the Inhomogeneous Electron Gas. *Phys. Rev. B* **1986**, *33*, 8822–8824. <https://doi.org/10.1103/PhysRevB.33.8822>.
6. (a) Grimme, S.; Antony, J.; Ehrlich, S.; Krieg, H. A Consistent and Accurate Ab Initio Parametrization of Density Functional Dispersion Correction (DFT-D) for the 94 Elements H-Pu. *J. Chem. Phys.* **2010**, *132*, 154104. <https://doi.org/10.1063/1.3382344>. (b) Grimme, S.; Ehrlich, S.; Goerigk, L. Effect of the Damping Function in Dispersion Corrected Density Functional Theory. *J. Comput. Chem.* **2011**, *32*, 1456–1465. <https://doi.org/10.1002/jcc.21759>.
7. Neese, F. A Critical Evaluation of DFT, Including Time-Dependent DFT, Applied to Bioinorganic Chemistry. *J. Biol. Inorg. Chem.* **2006**, *11*, 702–711. <https://doi.org/10.1007/s00775-006-0138-1>.
8. Chai, J.-D.; Head-Gordon, M. Long-Range Corrected Hybrid Density Functionals with Damped Atom–Atom Dispersion Corrections. *Phys. Chem. Chem. Phys.* **2008**, *10*, 6615. <https://doi.org/10.1039/b810189b>.
9. Weigend, F.; Ahlrichs, R. Balanced Basis Sets of Split Valence, Triple Zeta Valence and Quadruple Zeta Valence Quality for H to Rn: Design and Assessment of Accuracy. *Phys. Chem. Chem. Phys.* **2005**, *7*, 3297. <https://doi.org/10.1039/b508541a>.
10. (a) Orville, A.M.; Lipscomb, J.D. Binding of Isotopically Labeled Substrates, Inhibitors, and Cyanide by Protocatechuate 3,4-Dioxygenase. *J. Biol. Chem.* **1989**, *264*, 8791–8801. [https://doi.org/10.1016/S0021-9258\(18\)81863-4](https://doi.org/10.1016/S0021-9258(18)81863-4). (b) Whittaker, J.W.; Lipscomb, J.D.; Kent, T.A.; Münck, E. Brevibacterium Fuscum Protocatechuate 3,4-Dioxygenase. Purification, Crystallization, and Characterization. *J. Biol. Chem.* **1984**, *259*, 4466–4475. [https://doi.org/10.1016/S0021-9258\(17\)43071-7](https://doi.org/10.1016/S0021-9258(17)43071-7).

Disclaimer/Publisher’s Note: The statements, opinions and data contained in all publications are solely those of the individual author(s) and contributor(s) and not of MDPI and/or the editor(s). MDPI and/or the editor(s) disclaim responsibility for any injury to people or property resulting from any ideas, methods, instructions or products referred to in the content.